Ultrasound in Med. & Biol., Vol. 36, No. 7, pp. 1098–1108, 2010

0301-5629/$–see front matter

ELSEVIER

doi:10.1016/j.ultrasmedbio.2010.04.011

● *Original Contribution*

PROLONGED ENDOCHONDRAL BONE HEALING IN SENESCENCE IS SHORTENED BY LOW-INTENSITY PULSED ULTRASOUND IN A MANNER DEPENDENT ON COX-2

KOUJI NARUSE,* HIDEKI SEKIYA,[†,1] YOSHIHUMI HARADA,[‡] SADAHIRO IWABUCHI,[‡,2] YUSUKE KOZAI,[§] RYOTA KAWAMATA,[§] ISAMU KASHIMA,[§] KENTARO UCHIDA,* KEN URABE,* KANNICHI SETO,[†] MORITOSHI ITOMAN,* and YUKO MIKUNI-TAKAGAKI[¶]

*Department of Orthopedic Surgery, Kitasato University School of Medicine, Sagamihara; [†]First Department of Oral and Maxillofacial Surgery, School of Dental Medicine, Tsurumi University, Yokohama; [‡]Bone and Joint Research Laboratories, Teijin Pharma Limited, Tokyo; [§]Department of Maxillofacial Diagnostic Science; and [¶]Department of Functional Biology, Kanagawa Dental College, Yokosuka, Japan

(*Received* 22 *September* 2009; *revised* 15 *March* 2010; *in final form* 19 *April* 2010)

Abstract—To test whether mechanical loading produces faster healing in aged mice, fractured femurs of aged 1-year-old mice were subjected to low-intensity pulsed ultrasound (LIPUS), a treatment that is routinely used to help heal fractures in humans. Cyclooxygenase-2 knockout mice (COX-2$^{-/-}$), which lack an immediate early mediator of mechanical stimulation, were also studied by histochemistry, microcomputed tomography and quantitative polymerase chain reaction to determine the role of COX-2. The healing in the aged COX-2$^{-/-}$ mice is slow during the endochondral bone remodeling (>30 d), a period generally prolonged in senescence. For aged wild-type mice, LIPUS halved the endochondral phase to about 10 d, whereas that was not the case for aged COX-2$^{-/-}$ mice, which showed no apparent shortening of the prolonged endochondral-phase healing time. Injecting prostaglandin E_2 receptor agonists, however, rescued the COX-2$^{-/-}$ callus from insensitivity to LIPUS. In conclusion, COX-2 is a limiting factor in the delayed endochondral bone healing and is induced by LIPUS, which normalizes healing rate to the wild-type level. (E-mail: yukomtak@kdcnet.ac.jp) © **2010 World Federation for Ultrasound in Medicine & Biology.**

Key Words: **Cyclooxygenase-2 (COX-2), Prostaglandin E_2 (PGE_2), Fracture healing, Low-intensity pulsed ultrasound (LIPUS).**

INTRODUCTION

Fracture healing slows with age in rats (Ekeland et al. 1982) and humans (Nilsson and Edwards 1969). Recent investigation has shown that induced levels of COX-2 expression during the first postoperative week in the fracture callus of 1-year-old mice are only one-third of those of 8-week-old mice (Naik et al. 2009). Nonsteroidal antiinflammatory drugs (NSAIDs) and other COX-2 inhibitors have been reported to impair fracture healing in humans (Elmstedt et al. 1985; Sudmann and Hagen 1976) and animals (Bo et al. 1976). Significant osteogenic deficiencies were observed in rats aged 6–9 months that were administered indomethacin from the second postoperative week, whereas 2-month-old rats were not significantly affected (Elves et al. 1982). Thus, it was suggested that people who have fractured osteoporotic bone should avoid agents that inhibit COX-2 (Dinchuk et al. 1995).

Our previous studies established the role of COX-2 as a mechanical-response amplifier in primary rat bone cells and ST2 cells, a mouse stem cell line. COX-2 is an essential link in the process that sustains the anabolic effect of mechanical stimuli by amplifying the effect of the initial mechanical input as a result of biphasic secondary expression of COX-2 (Kawata and Mikuni-Takagaki 1998; Naruse et al. 2003). In fact, appropriate mechanical loading has a vital positive influence on skeletal healing (Augat et al. 2005). Therefore, to evaluate the efficacy of mechanical treatment with low-intensity pulsed ultrasound (LIPUS) in 1-year-old COX-2 knockout mice and their wild-type (WT) littermates, we examined their fracture calluses with and without LIPUS exposure.

Address correspondence to: Yuko Mikuni-Takagaki, Ph.D., Department of Science, Kanagawa Dental College, 82 Inaokacho, Yokosuka, Kanagawa 238-8580 Japan. E-mail: yukomtak@kdcnet.ac.jp

Present addresses: [1]Department of Oral Surgery, School of Medicine, Toho University, Tokyo and [2]Division of Immunoregulation, Institute for Genetical Medicine, Hokkaido University, Sapporo, Japan.

MATERIALS AND METHODS

Experimental design

We bilaterally fractured the femurs of aged (1-year-old) COX-$2^{-/-}$ mice and the WT littermates (COX-$2^{+/+}$). The right femur of each animal received a 20-min LIPUS treatment every day, starting on day 5, the fifth day after surgery (we define the day of surgery to be day 0). The left femurs served as controls and received mock treatment. Each group initially consisted of eight animals. In spite of the inherent risk of anesthesia, no more than two mice in each group died during these experiments. Three repeated experiments were performed. The time frame for the fracture healing of the aged mice, as well as that of skeletally mature, 10-week-old adult mice, is depicted in Fig. 1. The duration of endochondral bone formation is marked with double-headed arrows on a solid gray line for WT mice and a dotted gray line for the knockout mice.

To confirm whether prostaglandin E_2 (PGE_2) receptor agonists restore signals in response to LIPUS missing in old COX-$2^{-/-}$ mouse callus, we attempted a rescue experiment in which the bilateral femurs of the eight experimental knockout mice were fractured and treated with the EP-2 and EP-4 PGE_2 receptor agonists starting on day 5, the end of the inflammation stage, to day 21. Control COX-$2^{-/-}$ mice received vehicle solution. The right femur of each animal received a 20-min LIPUS treatment every day, starting on day 5.

Mice

The Animal Care and Use Committee of Kanagawa Dental College approved our experimental protocol. We used 48 mice. All mice were the hybrid C57BL/6J×129S7 (B6, 129S7-Ptgs2tm1Jed; The Jackson Laboratory, Bar Harbor, ME, USA) (Dinchuk et al. 1995), having been intercrossed for ~30 generations at Kanagawa Dental College. In addition to the knockout mice and the WT littermates, some heterozygous mice (COX-$2^{+/-}$) for the COX-2 gene were also used to histologically compare the healing rates.

Fractures

We anesthetized all mice with 80 mg/kg ketamine and 16 mg/kg xylazine and performed a medial parapatellar arthrotomy to insert a 26g needle into the medullary canal of the one or both femurs. After the exposed portion of the needle was cut off, the patella was replaced and the incision was sutured with 8-0 synthetic absorbable stitches. The stabilized femur was fractured manually at the midpoint of the diaphysis (Bonnarens and Einhorn 1984). Fracture healing was monitored by soft X-ray contact micrography (HA-60 system, Hitex Co., Osaka, Japan) of the femora of anesthetized mice with Industrial X-ray film IX FR (Fuji Photo Film Co. Ltd., Tokyo, Japan).

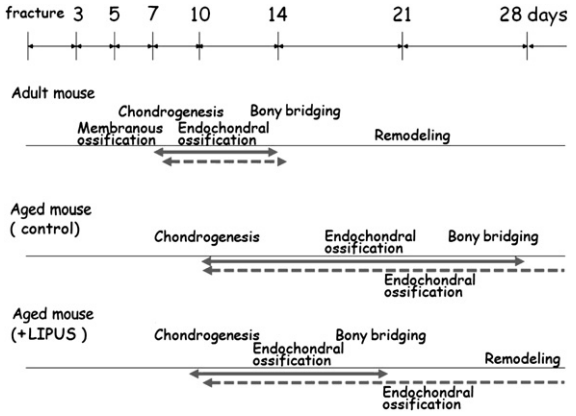

Fig. 1. Schematic representation of sequence of fracture healing processes in adult (10-week-old) and aged (1-year-old) mice. *Filled arrows* represent endochondral ossification stage in WT mice, and *dotted arrows* in COX-$2^{-/-}$ mice. Healing processes proceeded similarly in the 10-week-old COX-$2^{-/-}$ and the WT mice (See Supplementary Fig. S1 for radiographs).

Ultrasound treatment

A device equipped with six lead zirconate titanate transducers 13 mm in diameter (Teijin, Tokyo, Japan) applied LIPUS to the experimental fractures. The six transducers were connected to a generator through six separate lines with individual switches. A function generator (model HP33120A; Hewlett-Packard Japan, Ltd., Tokyo, Japan) produced a 200-μsec burst of 1.5-MHz sine waves repeated at 1.0 KHz at a spatial average and temporal average intensity of 30 mW/cm^2. These transcutaneous LIPUS parameters are identical to those used in human therapy (Fujioka et al. 2000), in experiments with rodents (Azuma et al. 2001) and in experiments with bone-cell cultures (Naruse et al. 2000, 2003). During treatment, the mice were anesthetized to aim the ultrasound to the fracture site with a subcutaneous injection of ketamine (80 mg/kg) and xylazine (16 mg/kg) and kept in a prone position on cylindrical holders with transducers placed close to the skin at the femoral fracture site, which was shaved and covered with ultrasound gel (Nippon Kohden, Tokyo, Japan) (Azuma et al. 2001). Control animals were also anesthetized and had transducers attached to the fracture site, but the transducers were not connected to the ultrasound generator.

Microfocused X-ray computed tomography

Microfocused X-ray computed tomography (micro-CT) equipped with a microfocus X-ray tube (focus size 8 × 8 μm, MCT-100MF, Hitachi Medical Corporation, Tokyo, Japan) produced a 3-D image of each femur from 200 image slices. The tube voltage, tube current,

magnification, and voxel size were 70 kV, 100 mA, x7 and 17.8 × 17.8 × 17.8 micrometers, respectively. Using TRI/3D BON software (Ratoc System Engineering Co. Ltd., Tokyo, Japan), 3-D structural parameters such as bone volume (BV, mm^3), bone surface (BS, mm^2), bone volume fraction (BV/TV, %), trabecular thickness (Tb.Th, μm), trabecular number (Tb.N, 1/mm) and trabecular separation (Tb.Sp, μm) were calculated (Ruegsegger et al. 1996). For the bone regions, we separated trabecular bone from cortical bone by 3-D space filtration; data from the each slice were converted to binary data using a threshold obtained by a discriminant analysis in which the pixel value histograms of background and bone were assumed to be normally distributed. We then chose each threshold as an intermediate pixel value lying on the tails of the two normal distributions.

Tissue preparation

For histochemical studies, resected calluses were immediately treated with 10% formalin at 0 °C, immersed overnight in fresh formalin and decalcified in 3M ethylenediamine tetraacetic acid for 2–3 weeks. Undecalcified 7-μm sections were prepared by embedding the callus in 2-hydroxyethylmethacrylate (GMA) and staining with classical hematoxylin/eosin, Goldner's trichrome or Toluidine blue.

Message levels in fracture calluses

Some fracture calluses were exposed to LIPUS for 20 min on days 6 and 7, 24 h apart. Femurs, both experimental and control, were excised 30 min after the last LIPUS exposure and immediately placed in RNA Later (Ambion, Austin, TX, USA). After dissection under a stereomicroscope, calluses were pulverized with a stainless steel mortar and pestle that had been chilled in liquid N_2 (Cryo-Press crusher; Microtec, Funabashi, Japan). Pulverized tissue was collected into a reagent containing phenol and guanidinium isothiocyanate to recover RNA. Total RNA was separated by centrifugation in Phase Lock Gel tubes (Eppendorf, Hamburg, Germany) after mixing with chloroform. Aliquots of 5 μg of recovered RNA were reverse-transcribed. The product cDNA was normalized with glyceraldehyde-3-phosphate dehydrogenase and subjected to conventional polymerase chain reaction (PCR) or real-time qPCR (QuantiTect SYBR Green PCR reagent kit; Qiagen, Hilden, Germany). Primer sequences are available upon request.

Injection of EP-2/EP-4 receptor agonists

From days 6–21, we subcutaneously injected two receptor agonists daily near the fracture callus in eight mice. The daily dose included 5 μg/kg of ONO-AE1-259-01, an EP-2 receptor agonist, dissolved in ethanol at 0.5 mg/mL and 5 μg/kg of ONO-AE1-329, an EP-4 receptor agonist, dissolved in water at 1 mg/mL. Both of these (a kind gift from Ono Pharmaceutical, Osaka, Japan) were further diluted to 5 μg/mL each in physiological saline solution containing 0.1% (w/v) Tween 80. Animals received 50 to 60 μL depending on body weight.

Statistical analysis

Relative values for the callus mRNAs are presented as the means ± SD for 6–8 rats in each group. Given the broad range of values detected among specimens from different calluses and different genetic groups, values relative to that of day 7 WT control callus in the same set of experiments were subjected to statistical analysis by Dennett's test with day 7 WT control value as a reference. Probability values less than 0.05 were considered significant. Because of the extremely low level on day 7 in WT control callus (VEGFa and MMP-3) and in KO callus (MMP-3), the results for VEGFa and MMP-3 are expressed without significance.

RESULTS

Fracture healing for aged mice

In the soft-X-ray profiles of femora of live and anesthetized 1-year-old mice taken on days 21 and 49, the blind observers detected differences between the profiles of knockout mice and those of WT mice (Fig. 2A). By day 49, all fractures in WT animals had reached union, whereas none of the fractures in knockout mice had done so. At both 21 d and 49 d, there was noticeably less healing of fractures in knockout mice than in WT mice. The fracture healing rate for heterozygotes (COX-$2^{+/-}$, Fig. 2A, c and d) was less than that of WT mice (Fig. 2Ae and 2Af) and greater than that of knockout mice (Fig. 2Aa and 2Ab). No less healing of fractures is present with younger, 10-week-old adult COX-$2^{-/-}$ mice (Supplementary Fig. S1 for comparison).

Effect of LIPUS on the rate of fracture healing in the aged mice

In the right femora of day 21 aged mice, Goldner's trichrome staining showed that LIPUS treatment from days 5–21 accelerated healing in both WT mice, which shifted from the endochondral ossification phase into the remodeling phase to cortical bone (Fig. 2Be to 2Bf), and the heterozygous COX-$2^{+/-}$ mice, which shifted from the bony callus phase with a fracture gap to the bony bridging phase by continuous woven bone (Fig. 2Bc to 2Bd).

In contrast, LIPUS is apparently ineffective for bony bridging in the healing of the COX-$2^{-/-}$ knockout mouse; Fig. 2Bb and 2Ba presented similar gaps at the fracture sites without being connected by woven bone. It should be noted that red staining represents the areas of soft tissue

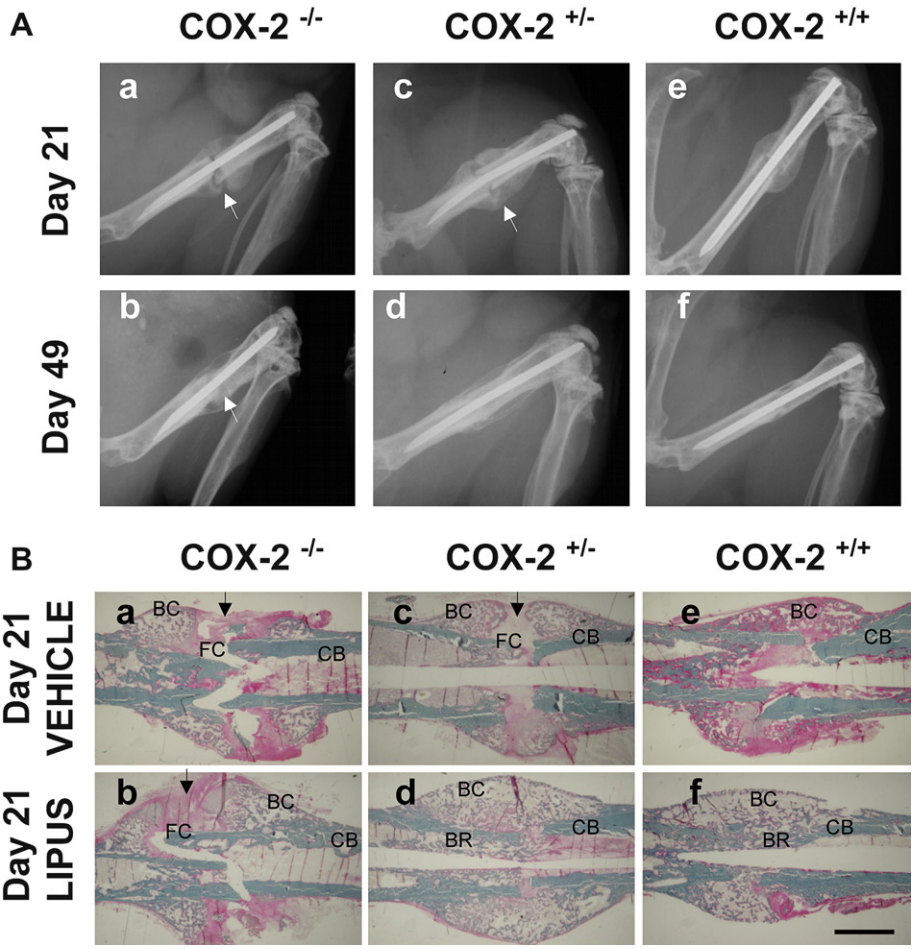

Fig. 2. Representative soft X-ray profiles (A) and histochemical profiles (B) of postfracture femurs of 1-year-old homozygous COX-2 knockout (COX-$2^{-/-}$), heterozygous (COX-$2^{+/-}$) and WT (COX-$2^{+/+}$) mice. (A) Day 21 (a, c, e) and day 49 (b, d, f) results are compared. (B) The day 21 postfracture femurs were either treated with LIPUS (b, d, f) or vehicle-treated (a, c, e). Undecalcified resin sections were visualized by Goldner's trichrome staining as described in Materials and Methods. Before the bony bridging typically observed in f and d, the edges of the newly formed woven bone are separated by the soft tissue as shown in a, b and c. FC, fibrous callus; BC, bony callus; CB, cortical bone; BR, area of bone remodeling. Scale bar represents 1 mm. Arrows in (A) and (B) indicate the fracture gaps filled with fibrous materials.

and slightly mineralized woven bone, and blue staining represents cortical bone. Calluses were further studied by Toluidine blue staining, which shows cartilage as purple, on earlier days 10 and 21. Chondrogenesis is at its peak and endochondral bone formation starts at about day 10 in aged normal mice. COX-$2^{-/-}$ and COX-$2^{+/+}$ calluses showed that cartilage formation in the knockout mice was essentially normal up to day 10 (Fig. 3Aa similar to 3Ac). However, exposure to LIPUS, which markedly accelerated endochondral replacement of cartilaginous tissue by woven bone in WT fractures (Fig. 3Ad *vs.* 3Ac), did not affect knockout fractures (Fig. 3Ab similar to 3Aa, rather than to 3Ad). By day 21, in control WT callus, most cartilage had been replaced by woven bone (Fig. 3Bc). LIPUS exposure accelerated remodeling furthermore by resorption of woven bone and cortical bone recovery (Fig. 3Bd). In knockout mice, however, endochondral bone formation was stunted, and cartilage was still apparent on day 21 (Fig. 3Ba). Even with LIPUS treatment, gaps filled with fibrous material persisted and prevented bony bridging (Fig. 3Bb). Overall, only in the presence of COX-2, LIPUS halved the interval needed for the endochondral bone formation of aged mice judged by the landmarks of healing, which is summarized in Fig. 1.

For the structural analysis of the newly formed bone, we obtained micro-CT scans of the femora on day 21. These image sets show the microstructural differences between fractures in knockout mice and those in their wild-type littermates, both with and without LIPUS (Fig. 3C). In the COX-$2^{-/-}$ femora, no bridging of bony callus was seen and fracture gaps

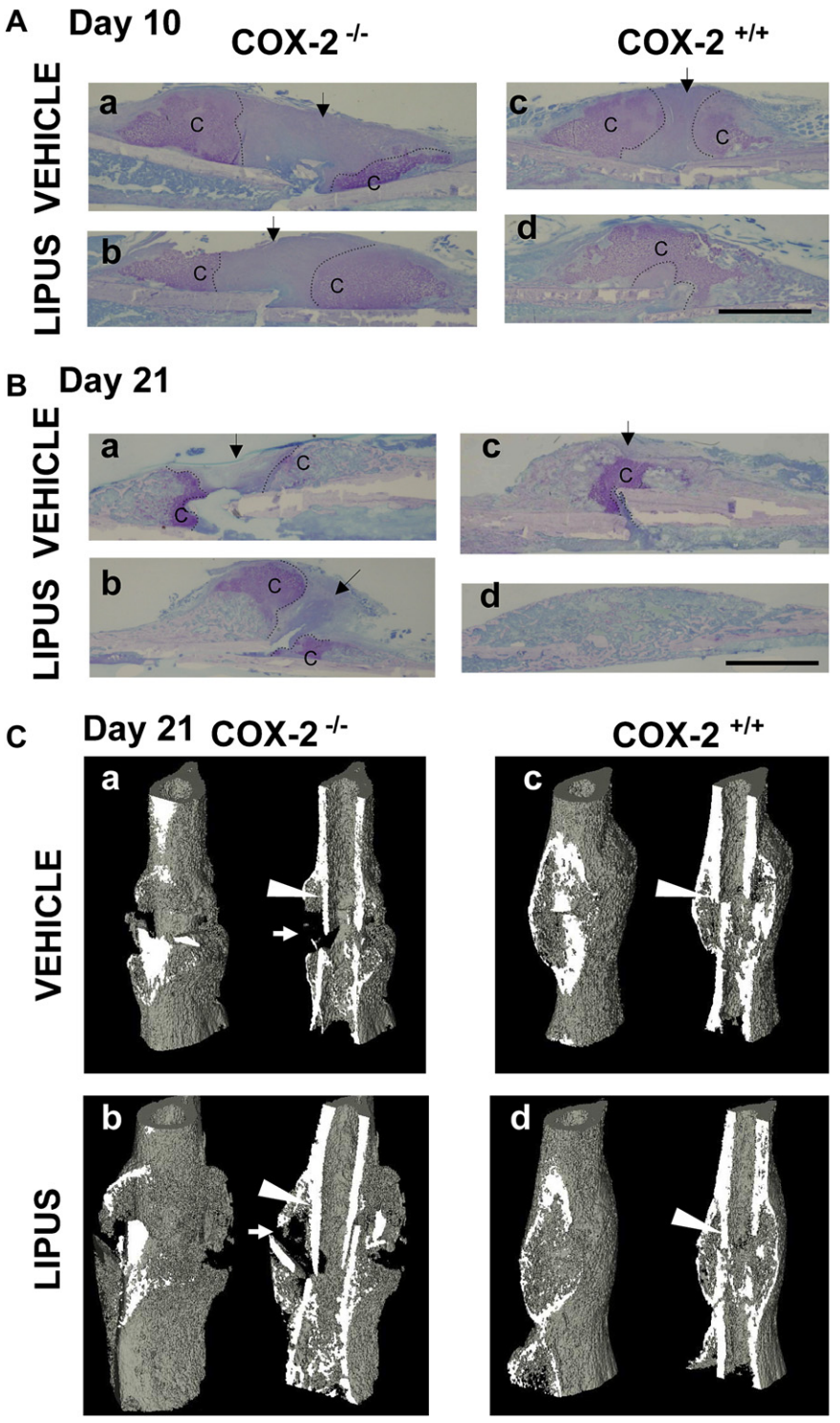

Fig. 3. Histochemical evaluation of fracture healing of 1-year-old mouse femora. (A) Toluidine blue staining profiles of day 10 postfracture femora of knockout mice (COX-$2^{-/-}$, a and b) and WT littermates (COX-$2^{+/+}$, c and d) were either LIPUS-exposed (b and d) or vehicle-treated (a and c). *Dotted lines* indicate the border of cartilaginous and fibrous callus. Chondroitin sulfate in cartilage (c) is stained purple. Scale bar: 1 mm. (B) Toluidine Blue staining profiles on day 21 under the same conditions as in Fig. 3A. (C) 3-D reconstruction of micro-CT profiles from day 21 postfracture femora of 1-year-old knockout mice (COX-$2^{-/-}$, a and b) and wild-type littermates (COX-$2^{+/+}$, c and d), either LIPUS-exposed (LIPUS, b and d) or vehicle-treated (Vehicle, a and c). Projections of reconstructed femora are depicted as projected at 30° clockwise to the frontal plane. Tomograms (*right*) and aspects (*left*) were reconstructed for representative femora. *Arrows* in (A), (B) and (C) indicate the fracture gaps, and the arrowheads in (C) represent the area of woven bone analyzed in Table 1.

were apparent regardless of LIPUS. At the fracture line, the bony callus curled inward, leaving a gap between the blunt ends of woven bone. In day 21 images of WT mice, however, healing had progressed such that the fracture line was undetectable and the periosteal membranous bone, as well as the woven bone, had fully bridged the fracture. Furthermore, LIPUS treatment markedly accelerated union of newly formed cortical bone, woven bone having mostly been resorbed by day 21 (Fig. 3Cd). Micro-CT analysis of the area of woven bone confirmed, on the basis of decreased BV/TV, trabecular thickness and increased trabecular separation, that resorption had progressed in mice exposed to LIPUS (Table 1). The BV/TV value, for example, was 26.2 ± 1.4% (see the area of woven bone indicated by an arrowhead in Fig. 3Cc) in the WT control callus, whereas the remaining woven bone in the LIPUS-exposed, resorbed callus (Fig. 3Cd equivalent to Fig. 3Bd) was 20.8 ± 0.3%. In contrast, in day 21 images of the femora of knockout mice, LIPUS brought little apparent change; cartilage and the fracture gap persisted. There was, however, a thickening of woven bone (Fig. 3Bb and 3Cb *vs.* 3Ba and 3Ca) that correspond to the micro-CT data of increased BV/TV, 26.4 ± 1.4% *vs.* 21.1 ± 0.7%; increased trabecular number, 8.1 ± 0.6 mm^{-1} *vs.* 6.4 ± 0.5 mm^{-1}; and decreased trabecular separation, 91.0 ± 8.9 μm *vs.* 123.1 ± 11.0 μm (Table 1). These values in the LIPUS-exposed knockout callus just happened to be similar to the WT vehicle value.

Bone and cartilage-protein expression in callus

To further delineate the mechanisms causing the slower healing rate, we selected messages that characterize bone healing. Dissected calluses were subjected to reverse transcriptase–PCR. By comparing results of basal day 7 (Fig. 4A, lane D7), day 7 after LIPUS (lane D7US) and basal day 10 (lane D10), the effect of LIPUS was evaluated in the normal course of events. In Fig. 4Aa1–4Aa3, levels of Col1a1, Col2a1, osterix, alkaline phosphatase (ALP), aggrecan and BMP-6 all increased in the order D7≤D7US<D10 (for Runx2 in Fig. 4A, b, D7<D7US≒D10). MMP-13 and osteocalcin showed similar profiles (data not shown). The order for the level of MMP-9 was reversed (Fig. 4Ac, D7≥D7US≥D10). On the other hand, WT D7US MMP-2 level was much higher with LIPUS than D7 and D10 basal levels (Fig. 4Ad, D7US>D7≒D10; TGF-α1 was similar). D7US levels of Col10a1, BMP-2, BMP-4, FGF-2, VEGFa, MMP-3, COX-2 and RANKL were also higher than both D7 and D10 basal levels (Fig. 4Ae to 4Ah). Compared with these LIPUS-specific WT responses in 4Ad–4Ah, Col3a1 and COX-1 remained constant throughout (Fig. 4Ai). In COX-$2^{-/-}$ callus on day 7 (Fig. 4B), in contrast, loss of detectable messages was observed for VEGFa, ALP and MMP-9 (TGF-α2 and RANKL showed similar results), regardless of LIPUS (Fig. 4Ba). In BMP-6, as well as MMP-2 and aggrecan, lower levels of expression were detected in the knockout callus, especially with LIPUS (WT>KO>KOUS, Fig. 4Bb). BMP-2, COL1a1, COL1a2 and COL3a1, as well as Runx2 and osterix messages in COX-$2^{-/-}$ mouse callus, showed similar levels to the WT day 7 levels (Fig. 4Bc). MMP-3 (Fig. 4Bd), Col10a1 and possibly TGF-α1and BMP-4 (Fig. 4Be) increased the messages in knockout callus, especially after LIPUS exposure (WT<KO<KOUS). The level of FGF-2 message in the knockout mouse was higher than the WT but showed no further elevation by LIPUS (WT<KO≒⋆KOUS in Fig. 4Bf).

Rescue from deficient healing with EP-2/EP-4 receptor agonists

Micro-CT profiles and parameters show that the 1-year-old COX-$2^{-/-}$ mice healed just as well as their WT littermates if EP-2 and EP-4 receptor agonists were present. Table 2 and Fig. 5, compared with Table 1 and Figs. 3 and 4, showed the regained WT-level response to LIPUS in addition to the recovery of parameters to the WT levels in EP-2/EP-4–treated COX-$2^{-/-}$ mice callus; Fig. 5Ab and 5Bb *vs.* 5Aa and 5Ba are equivalent

Table 1. Effects of LIPUS on structural parameters of newly formed woven bone in the external callus analyzed in the day 21 fractures by 3-D micro-CT

	WT littermates		Knockout	
Variable	Vehicle	LIPUS	Vehicle	LIPUS
BS/BV 1/mm	61.4 ± 2.9	65.1 ± 2.3*†	60.7 ± 2.8	61.2 ± 1.6
BV/TV%	26.2 ± 1.4	20.8 ± 0.3*†	21.1 ± 0.7*	26.4 ± 1.4†
Tb.Th μm	32.6 ± 0.9	30.8 ± 1.4*†	32.8 ± 1.5	32.6 ± 0.8
Tb.N 1/mm	8.1 ± 0.8	6.8 ± 0.2	6.4 ± 0.5*	8.1 ± 0.6†
Tb.Sp μm	91.6 ± 8.0	116.9 ± 2.9*†	123.1 ± 11.0*	91.0 ± 8.9†
Fractal dimension	2.25 ± 0.0	2.19 ± 0.0	2.31 ± 0.06	2.31 ± 0.01

Wild-type (Cox-$2^{+/+}$) and COX-2KO (Cox-$2^{-/-}$) mouse calluses were subjected to the analysis.

Values are mean ± SD. Within each variable, significance was compared with vehicle for the WT mice (*$p < 0.05$), and within each genotype, significance was compared with LIPUS-untreated vehicle mice (†$p < 0.05$) by the two-tailed multiple *t*-test with Bonferroni correction (4 comparisons in 4 groups).

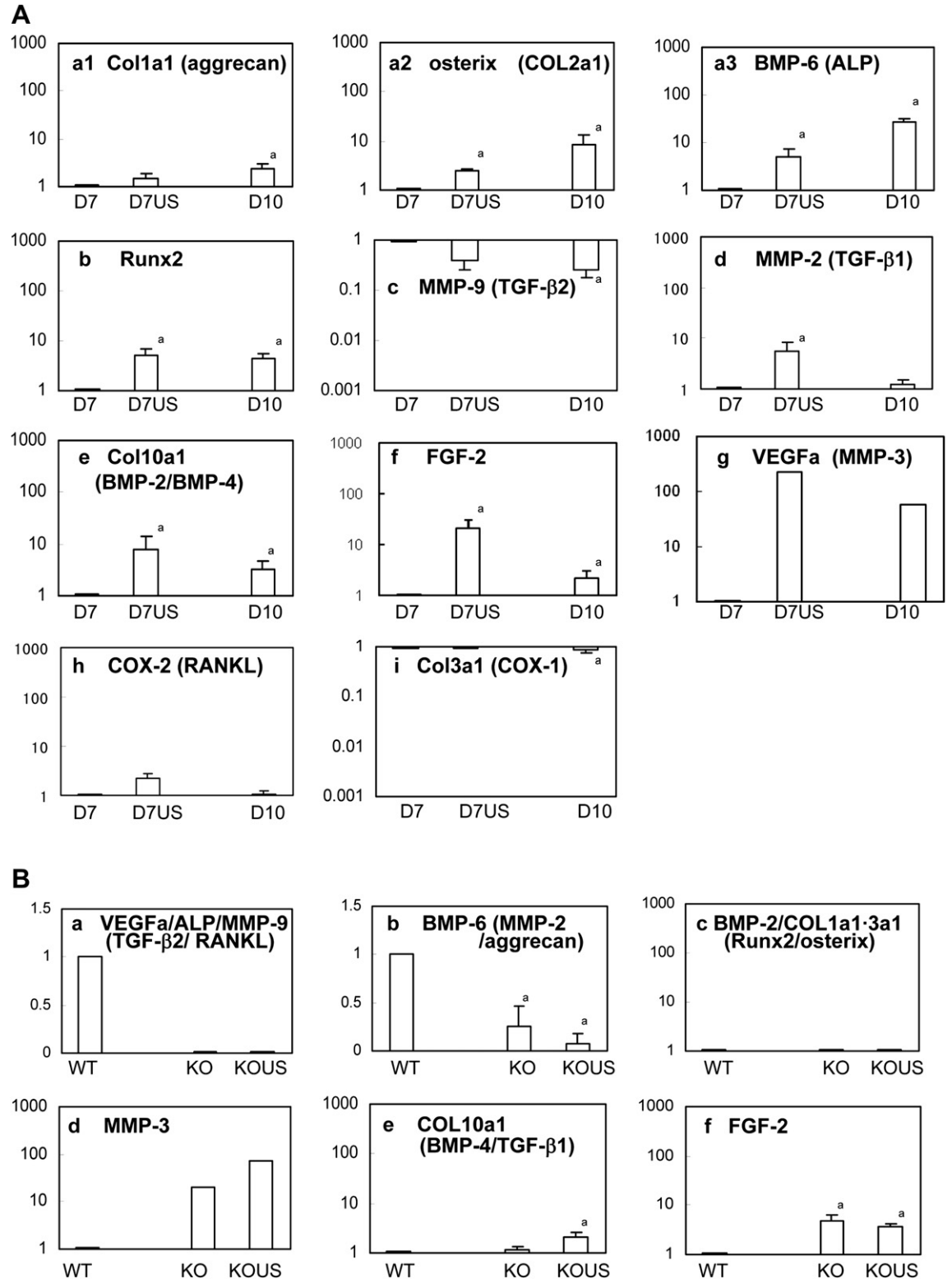

Fig. 4. Transcript levels in the fracture callus of 1-year-old mice. (A) WT littermates, D7, D7US and D10, at 7 or 10 d post-fracture. D7US samples were from day 7 femurs exposed to LIPUS; D7 and D10, vehicle-treated controls from day 7 and day 10 femurs. Total RNA was extracted from the dissected callus and subjected to quantitative reverse transcriptase–PCR as described in Materials and Methods. In a1, Col1a1 (similar to aggrecan); a2, osterix (similar to Col2a1) a3, BMP-6 (similar to ALP); b, Runx2; c, MMP-9 (similar to TGF-α2); d, MMP-2 (similar to TGF- α1); e, Col10a1 (similar to BMP-2 and BMP-4); f, FGF-2; g, VEGFa (similar to MMP-3); h, COX-2 (similar to RANKL); i, Col3a1 (similar to

to Fig. 3Bd and 3Cd *vs.*3Bc and 3Cc, and Fig. 5C is equivalent to Fig. 4Ag.

DISCUSSION

Although LIPUS accelerates the healing process for WT 1-year-old mice, it does not do so for their COX-$2^{-/-}$ littermates. The significantly retarded fracture healing rate we observed for aged COX-$2^{-/-}$ mice during the endochondral ossification accords well with previously published reports that NSAIDs and other COX inhibitors slowed down the fracture healing process in adult rats and humans (Allen et al. 1980; Bo et al. 1976; Elmstedt et al. 1985; Sudmann and Hagen 1976) and that a single local application of a retroviral vector expressing a single COX-2 transgene accelerated fracture healing in aged rats (Rundle et al. 2008).

Because the healing milestones during and after the endochondral bone formation are essentially the same for 10-week-old COX-$2^{-/-}$ as they are for their WT littermates (see summary in Fig. 1 and Supplementary Fig. S1), the question to be asked is what function COX-2 and its product PGE_2 perform in fracture healing, specifically in older animals. Keller et al. (1993) observed significant stimulation of endochondral remodeling into bone after infusing PGE_2 into 9-month-old rabbits from weeks 3–6 postfracture. However, no significant difference was observed if the same infusion was given during the first three weeks. They suggested that PGE_2 is scarce and that if artificially infused in later weeks, it effectively promotes remodeling. In our present experiment, LIPUS exposure accelerated the rate of endochondral remodeling in the aged WT mice. Although COX-2 may not be the sole determinant of fracture healing, mechanical stimulation such as LIPUS increases the amount or level of PGE_2 in aged individuals as a result of an increase in COX-2, which is induced in mechanically stimulated osteoblasts (Forwood 1996; Naruse et al. 2003). Feedback upregulation of COX-2 by the product, PGE_2 (Kawaguchi et al. 1994), explains the long-lasting effect of exercise on PGE_2 production and bone formation (Forwood 1996; Naruse et al. 2003).

Previous *in vivo* studies have demonstrated that LIPUS affects all phases of the healing process in rats and that LIPUS shortens the healing period in patients (Azuma et al. 2001; Nelson et al. 2003). Yang et al. (1996) reported in adult rats a biphasic shift in aggrecan gene expression to a significantly higher level on day 7 and a lower level on day 21. These changes are anticipated if the effect of LIPUS on aggrecan gene is the result of attaining earlier landmarks and final union. In LIPUS-treated WT callus, we detected increases in ALP, Col2a1, aggrecan, Runx2, osterix and many other differentiation markers in the order D7<D7US≦D10, or decreases in the same order (MMP-9 and TGF-α2). Such changes induced by LIPUS are as anticipated in the due course of time and may have been attained by increasing circulation (Rawool et al. 2003) or slightly raising body temperature (Reuter et al.1984). In contrast, we discovered more specific effects provably dependent on each promoter in other genes of distinct behavior. Col10a1, BMP-2 and BMP-4 responded more specifically to LIPUS, judging from the higher levels of D7US than both D7 and D10 basal levels. MMP-2, MMP-3, TGF-α1, FGF-2, VEGFa, COX-2 and RANKL were elevated solely by LIPUS, suggestive of the specific target genes for specific healing effects. It should be noted that LIPUS specifically induces RANKL, which is essential to osteoclastogenesis and bone resorption (Tsukii et al.1998) and is not induced in COX-$2^{-/-}$ mouse callus. We found that LIPUS triggers additional metabolic turnover in fracture callus, even in aged mice, as long as PGE_2 is available. In COX-$2^{-/-}$ mice, lack of many such critical angiogenic and/or catabolic components as VEGFa and MMP-9 (Colnot et al. 2003; Engsig et al. 2000; Gerber et al. 1999), which have been reported being downstream of PGE_2 (Callejas et al. 2001; Gallo et al. 2001), prevents matrix degradation and remodeling in the healing bone. Fibroblastic Col3a1 messages, as well as those of Col1a1, remained constant in COX-$2^{-/-}$ callus, further supporting our observation of persistent mesenchymal tissue in the COX-$2^{-/-}$ fracture gaps regardless of LIPUS. In contrast to these mostly unaffected matrix proteins, Col10a1, BMP-4, TGF-α1 and possibly MMP-3 were upregulated in the COX-$2^{-/-}$ callus by LIPUS, suggesting certain compensatory alternative pathway(s) independent of COX-2. In addition, COX-$2^{-/-}$ callus showed persistent higher levels of FGF-2, which was reported to stimulate proliferation of fibroblasts and chondrocytes and to prolong the cartilaginous callus phase (Nakajima et al. 2001).

With regard to early-phase responses, Street et al. (2001) reported elevated VEGF and platelet-derived

COX-1). (B) Knockout mice, KO and KOUS, and WT littermates, WT, which is identical to D7 in (a), all at postfracture day 7. KO and WT values are basal controls. Panels a, VEGFa, ALP and MMP-9 (similar to TGF-α2 and RANKL); b, BMP-6 (similar to aggrecan and MMP-2); c, BMP-2, Col1a1, Col2a1and Col3a1 (similar to Runx2 and osterix); d, MMP-3; e, Col10a1 (similar to BMP-4 and TGF-α1); f, FGF-2. Data in (A) and (B) are expressed as the means ± SD. [a] Significant at $p < 0.05$ by Dennett's test with day 7 WT control values, D7 in (A) and WT in (B), as references. Fig. 4Ag and 4Bd, which have extremely low D7/WT values, are presented without SD values as described in Materials and Methods.

Table 2. Effects of LIPUS on structural parameters of newly formed woven bone in the external callus analyzed in the day 21 fractures by 3-D micro-CT

	WT littermates*		Knockout with EP2/EP4 agonists	
Variable	Vehicle	LIPUS	Vehicle	LIPUS
BS/BV 1/mm	61.4 ± 2.9	65.1 ± 2.3†‡	61.9 ± 0.7	70.7 ± 5.2†‡
BV/TV%	26.2 ± 1.4	20.8 ± 0.3†‡	27.1 ± 2.2	21.1 ± 2.5†‡
Tb.Th μm	32.6 ± 0.9	30.8 ± 1.4†‡	32.2 ± 0.4	28.2 ± 1.8†‡
Tb.N 1/mm	8.1 ± 0.8	6.8 ± 0.2	8.4 ± 0.6	7.5 ± 1.3
Tb.Sp μm	91.6 ± 8.0	116.9 ± 2.9†‡	86.7 ± 8.8	105.4 ± 4.2†‡
Fractal dimension	2.25 ± 0.0	2.19 ± 0.0	2.27 ± 0.01	2.30 ± 0.06

Results of COX-2 KO mice administered EP2 and EP4 agonists and of WT littermates were subjected to the analysis.

Values are mean ± SD. Within each variable, significance was compared with vehicle for the WT mice (†$p < 0.05$), and within each genotype, significance was compared with LIPUS-untreated vehicle mice (‡$p < 0.05$) by the two-tailed multiple t-test with Bonferroni correction (4 comparisons in 4 groups).

*Data from Table 1.

growth factor (PDGF) levels in plasma and fracture hematoma in fracture patients irrespective of age. Some other mechanisms must be sought, they wrote, for delayed union in elderly people. Also in rats, Meyer et al. (2001) reported transient upregulation of BMPs and PDGF immediately after fracture, regardless of age. We detected many specifically elevated genes in LIPUS-treated callus of 1-year-old WT mice that support the potential for aged mouse callus to respond to other types of mechanical stimulation as well. In the presence of COX-2, induced VEGFa will cause osteoblastic cells to differentiate, as reported by others (Peng et al. 2002; Street et al. 2002). Colnot et al. (2003) demonstrated that union is delayed in MMP-9 knockout mice and that MMP-9 mediates vascular invasion of cartilaginous callus. Absence of MMP-9 is responsible for the lack of VEGF

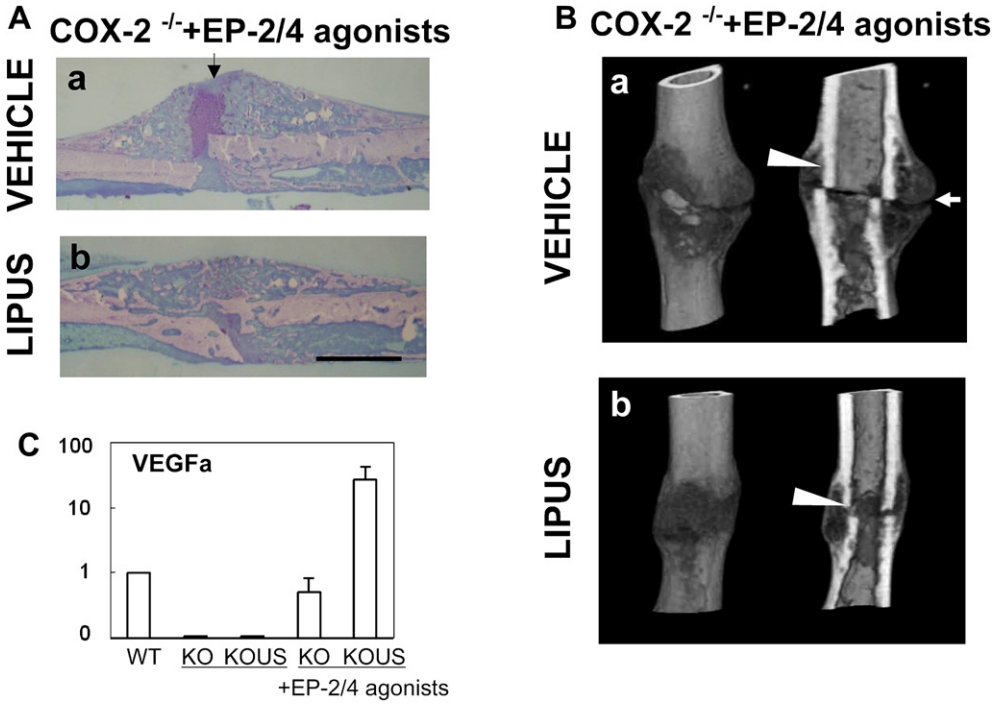

Fig. 5. Effects of EP-2 and EP-4 agonists and LIPUS on fracture callus of 1-year-old COX-2 knockout mouse femur. Histochemical (A) and micro-CT (B) profiles of callus with daily injections of agonists alone (a, Vehicle, from left femur) or with agonists and LIPUS exposure (b, LIPUS, from right femur). Daily treatments, started after 5 d postfracture, were continued through day 21. In (A) and (B), experimental conditions and markers in the figure are similar to those presented in Fig. 3. (C) Recovered expression of VEGFa in COX-$2^{-/-}$ fracture callus treated with EP-2/EP-4 agonists. Samples were analyzed under similar conditions to those described in Fig. 4 and relative values to that of the basal WT callus (WT) are presented.

bioavailability (Bergers et al. 2000). In COX-2$^{-/-}$ mice, neither VEGFa nor MMP-9 messages were detectable regardless of LIPUS. COX-2 is a ubiquitous upstream regulator of MMP-2, MMP-9, VEGF (Callejas et al. 2001; Gallo et al. 2001) and RANKL (Tsukii et al. 1998). Thus, our results underline the inability of COX-2$^{-/-}$ mice to use these molecules in fracture callus, even when mechanically stimulated.

COX-2 is essential in later stages of fracture healing in aged mice; cartilage and bone formation progress quasinormally in knockout mice up to day 10, and then they slow down. Recovery to the WT level was attained by injecting EP-2/EP-4 agonists after day 5. It is apparent that cells regained responsiveness to LIPUS. This COX-2$^{-/-}$ experiment to rescue normal bone formation and resorption, LIPUS-induced as well as basal, shows that the loss of COX-2–derived PGE_2 deters the endochondral remodeling of fractures in aged mice. It is possible that mechanical stimulation, which provides PGE_2 through COX-2 induction (Kawata and Mikuni-Takagaki 1998; Naruse et al. 2003), is less in aged mice than in younger mice during the endochondral remodeling phase of fracture healing. Elderly people receiving long-term NSAID therapy may have a slower healing rate because of the blockade of signal transduction downstream of mechanical loading, which favors skeletal healing (Augat et al. 2005).

Acknowledgments—We thank Kazuaki Miyagawa, presently at Osaka University Graduate School of Dental Medicine for technical assistance; Koji Tomimori and Dr. Yoshiaki Azuma, Teijin Pharma, for helpful discussions; and Dr. Ikuya Matsubara, Department of Science, Kanagawa Dental College for advice on the statistical analysis. This investigation was supported in part by grants-in-aid from the Ministry of Science, Education, and Culture of Japan to Y. M.-T. and H. S.; by grants-in-aid from the Ministry of Health, Labor, and Welfare for Research on the Human Genome, Tissue Engineering, and Food Biotechnology, to M. I.; and by a research support grant from Kanagawa Odontological Society to Y. M.-T.

SUPPLEMENTARY DATA

Supplementary data associated with this article can be found, in the online version, at doi:10.1016/j.ultrasmedbio.2010.04.011.

REFERENCES

Allen HL, Wase A, Bear WT. Indomethacin and aspirin: Effect of nonsteroidal anti-inflammatory agents on the rate of fracture repair in the rat. Acta Orthop Scand 1980;51:595–600.

Augat P, Simon U, Liedert A, Claes L. Mechanics and mechano-biology of fracture healing in normal and osteoporotic bone. Osteoporos Int 2005;16(Suppl. 2):S36–S43.

Azuma Y, Ito M, Harada Y, Takagi H, Ohta T, Jingushi S. Low-intensity pulsed ultrasound accelerates rat femoral fracture healing by acting on the various cellular reactions in the fracture callus. J Bone Miner Res 2001;16:671–680.

Bergers G, Brekken R, McMahon G, Vu TH, Itoh T, Tamaki K, Tanzawa K, Thorpe P, Itohara S, Werb Z, Hanahan D. Matrix metalloproteinase-9 triggers the angiogenic switch during carcinogenesis. Nat Cell Biol 2000;2:737–744.

Bo J, Sudmann E, Marton PF. Effect of indomethacin on fracture healing in rats. Acta Orthop Scand 1976;47:588–599.

Bonnarens F, Einhorn TA. Production of a standard closed fracture in laboratory animal bone. J Orthop Res 1984;2:97–101.

Callejas NA, Casado M, Diaz-Guerra MJ, Bosca L, Martin-Sanz P. Expression of cyclooxygenase-2 promotes the release of matrix metalloproteinase-2 and -9 in fetal rat hepatocytes. Hepatology 2001;33:860–867.

Colnot C, Thompson Z, Miclau T, Werb Z, Helms JA. Altered fracture repair in the absence of MMP9. Development 2003;130:4123–4133.

Dinchuk JE, Car BD, Focht RJ, Johnston JJ, Jaffee BD, Covington MB, Contel NR, Eng VM, Collins RJ, Czerniak PM. Renal abnormalities and an altered inflammatory response in mice lacking cyclooxygenase II. Nature 1995;378:406–409.

Ekeland A, Engesoeter LB, Langeland N. Influence of age on mechanical properties of healing fractures and intact bones in rats. Acta Orthop Scand 1982;53:527–534.

Elmstedt E, Lindholm TS, Nilsson OS, Tornkvist H. Effect of ibuprofen on heterotopic ossification after hip replacement. Acta Orthop Scand 1985;56:25–27.

Elves MW, Bayley I, Roylance PJ. The effect of indomethacin upon experimental fractures in the rat. Acta Orthop Scand 1982;53:35–41.

Engsig MT, Chen QJ, Vu TH, Pedersen AC, Therkidsen B, Lund LR, Henriksen K, Lenhard T, Foged NT, Werb Z, Delaisse JM. Matrix metalloproteinase 9 and vascular endothelial growth factor are essential for osteoclast recruitment into developing long bones. J Cell Biol 2000;151:879–889.

Forwood MR. Inducible cyclo-oxygenase (COX-2) mediates the induction of bone formation by mechanical loading in vivo. J Bone Miner Res 1996;11:1688–1693.

Fujioka H, Tsunoda M, Noda M, Matsui N, Mizuno K. Treatment of ununited fracture of the hook of hamate by low-intensity pulsed ultrasound: A case report. J Hand Surg [Am] 2000;25:77–79.

Gallo O, Franchi A, Magnelli L, Sardi I, Vannacci A, Boddi V, Chiarugi V, Masini E. Cyclooxygenase-2 pathway correlates with VEGF expression in head and neck cancer. Implications for tumor angiogenesis and metastasis. Neoplasia 2001;3:53–61.

Gerber HP, Vu TH, Ryan AM, Kowalski J, Werb Z, Ferrara N. VEGF couples hypertrophic cartilage remodeling, ossification and angiogenesis during endochondral bone formation. Nat Med 1999;5:623–628.

Kawaguchi H, Raisz LG, Voznesensky OS, Alander CB, Hakeda Y, Pilbeam CC. Regulation of the two prostaglandin G/H synthases by parathyroid hormone, interleukin-1, cortisol, and prostaglandin E2 in cultured neonatal mouse calvariae. Endocrinology 1994;135:1157–1164.

Kawata A, Mikuni-Takagaki Y. Mechanotransduction in stretched osteocytes—Temporal expression of immediate early and other genes. Biochem Biophys Res Commun 1998;246:404–408.

Keller J, Klamer A, Bak B, Suder P. Effect of local prostaglandin E2 on fracture callus in rabbits. Acta Orthop Scand 1993;64:59–63.

Meyer RA, Meyer MH, Phieffer LS, Banks DM. Delayed union of femoral fractures in older rats:decreased gene expression. BMC Musculoskelet Disord 2001;2:2.

Naik AA, Xie C, Zuscik MJ, Kingsley P, Schwarz EM, Awad H, Guldberg R, Drissi H, Puzas JE, Boyce B, Zhang X, O'Keefe RJ. Reduced COX-2 expression in aged mice is associated with impaired fracture healing. J Bone Miner Res 2009;24:251–264.

Nakajima F, Ogasawara A, Goto K, Moriya H, Ninomiya Y, Einhorn TA, Yamazaki M. Spatial and temporal gene expression in chondrogenesis during fracture healing and the effects of basic fibroblast growth factor. J Orthop Res 2001;19:935–944.

Naruse K, Mikuni-Takagaki Y, Azuma Y, Ito M, Oota T, Kameyama K, Itoman M. Anabolic response of mouse bone-marrow-derived stromal cell clone ST2 cells to low-intensity pulsed ultrasound. Biochem Biophys Res Commun 2000;268:216–220.

Naruse K, Miyauchi A, Itoman M, Mikuni-Takagaki Y. Distinct anabolic response of osteoblast to low-intensity pulsed ultrasound. J Bone Miner Res 2003;18:360–369.

Nelson FR, Brighton CT, Ryaby J, Simon BJ, Nielson JH, Lorich DG, Bolander M, Seelig J. Use of physical forces in bone healing. J Am Acad Orthop Surg 2003;11:344–354.

Nilsson BE, Edwards P. Age and fracture healing: a statistical analysis of 418 cases of tibial shaft fractures. Geriatrics 1969;24:112–117.

Peng H, Wright V, Usas A, Gearhart B, Shen HC, Cummins J, Huard J. Synergistic enhancement of bone formation and healing by stem cell-expressed VEGF and bone morphogenetic protein-4. J Clin Invest 2002;110:751–759.

Rawool NM, Goldberg BB, Forsberg F, Winder AA, Hume E. Power Doppler assessment of vascular changes during fracture treatment with low-intensity ultrasound. J Ultrasound Med 2003;22:145–153.

Reuter U, Strempel F, John F, Knoch HG. [Modification of bone fracture healing by ultrasound in an animal experiment model]. Z Exp Chir Transplant Kunstliche Organe 1984;17:290–297.

Ruegsegger P, Koller B, Muller R. A microtomographic system for the nondestructive evaluation of bone architecture. Calcif Tissue Int 1996;58:24–29.

Rundle CH, Strong DD, Chen ST, Linkhart TA, Sheng MH, Wergedal JE, Lau KH, Baylink DJ. Retroviral-based gene therapy with cyclooxygenase-2 promotes the union of bony callus tissues and accelerates fracture healing in the rat. J Gene Med 2008;10: 229–241.

Street J, Bao M, deGuzman L, Bunting S, Peale FV Jr, Ferrara N, Steinmetz H, Hoeffel J, Cleland JL, Daugherty A, van Bruggen N, Redmond HP, Carano RA, Filvaroff EH. Vascular endothelial growth factor stimulates bone repair by promoting angiogenesis and bone turnover. Proc Natl Acad Sci U S A 2002;99:9656–9661.

Street JT, Wang JH, Wu QD, Wakai A, McGuinness A, Redmond HP. The angiogenic response to skeletal injury is preserved in the elderly. J Orthop Res 2001;19:1057–1066.

Sudmann E, Hagen T. Indomethacin-induced delayed fracture healing. Arch Orthop Unfallchir 1976;85:151–154.

Tsukii K, Shima N, Mochizuki S, Yamaguchi K, Kinosaki M, Yano K, Shibata O, Udagawa N, Yasuda H, Suda T, Higashio K. Osteoclast differentiation factor mediates an essential signal for bone resorption induced by 1 alpha,25-dihydroxyvitamin D3, prostaglandin E2, or parathyroid hormone in the microenvironment of bone. Biochem Biophys Res Commun 1998;246:337–341.

Yang KH, Parvizi J, Wang SJ, Lewallen DG, Kinnick RR, Greenleaf JF, Bolander ME. Exposure to low-intensity ultrasound increases aggrecan gene expression in a rat femur fracture model. J Orthop Res 1996; 14:802–809.